A Digital Phase Locked Loop based System for Nakagami -m fading Channel Model

Basab B Purkayastha
Department of Electronics and Communication Technology, Gauhati University
Guwahati-781034, Assam, India

Kandarpa Kumar Sarma
Department of Electronics and Communication Technology, Gauhati University
Guwahati-781034, Assam, India

ABSTRACT
The modified structure of a Digital Phase Locked Loop (DPLL) based systems for dealing with Nakagami-m fading is proposed here. The emphasis of the work is to generate input signal under various fading conditions with certain modulation transmitted through Nakagami-m channels and to evaluate the performance of the proposed DPLL in terms of Bit Error Rate (BER). Statistical characteristics of the faded input signal have been evaluated in terms of Probability Distribution Function (PDF), Level Crossing Rate (LCR) and Average Fade Duration (AFD). A sixth order Least Square Polynomial Fitting (LSPF) block and Roots Approxiator (RA) for better phase-frequency detection have been implemented as a replacement of Phase Frequency Detector (PFD) and Loop Filter (LF) of a traditional DPLL, which has helped to attain optimum performance of DPLL. The results of simulation of the proposed DPLL with Nakagami –m fading and QPSK modulation shows that the proposed method provides better performance than existing systems of similar type.

Keywords
digital phase locked loop, numerically controlled oscillator, nakagami –m fading channels, least square polynomial fitting filter, level crossing rate and average fade duration.

1. INTRODUCTION
The Phase Locked Loop (PLL) is a device which generates a clock and synchronizes it with an input signal. The input signal can be data or another clock. PLLs generate stable frequencies, recover a signal from a noisy communication channel, or distribute clock timing pulses in digital logic designs such as microprocessors.

In recent years coherent communication systems for phase tracking purposes have employed DPLLs. This is primarily due to the fact that digital systems are more reliable, compact, and efficient than analog systems [1, 2, 3, 4, 5, 6]. There are several different methods of digitally determining the phase difference between two waveforms. Some of these methods are better suited to hardware than software and vice versa. Here, we present a phase detection technique based on Least Square Polynomial Fitting (LSPF) and Roots Approximation.

The importance of considering a fading received signal is apparent in the design and analysis of communication systems. In the literature, many models of fading channel have been discussed and researched [7, 8]. Signal fading can drastically affect the performance of fading terrestrial communication systems. Fading caused by multipath propagation can degrade the bit-error-rate (BER) performance of a digital communication system resulting data loss or dropped calls in a cellular system. So it is essential to understand the nature of multipath phenomenon and how to anticipate when such phenomenon occurs in order to improve radio performance.

The Nakagami−m distribution has gained widespread application in the modeling of physical fading radio channels. The primary justification of the use of Nakagami−m fading model is its good fit to empirical fading data. It is versatile and through its parameter m, we can model signal fading conditions that range from severe to moderate, to light fading or no fading. In other words, Nakagami-*m* model is a generalized model and the models such as Rayleigh, Racian etc. are the special cases of the Nakagami -*m* fading model.

The design of DPLL for coherent carrier detection presented in this paper is based on polynomial fitting and corresponding roots approximation algorithm using uniform sampling under consideration that the receiver has complete knowledge of the transmitted and the received signals despite corrupted both by channel and fading conditions. We present here a DPLL based system for dealing with Nakagami -*m* fading.

Section 2 of this paper describes the operation of various blocks of the proposed DPLL. A brief discussion has been made on QPSK signal modeling and Nakagami –m channel modeling in Section 3. Experimental considerations have been discussed in Section 4. Section 5 deals with results and performance of the system. Finally conclusions have been made in Section 6.

2. PROPOSED DIGITAL PHASE LOCKED LOOP
The proposed DPLL is designed for carrier detection from noisy multipath faded signal and has three major components. Namely, Least Square Polynomial Fitting Block (LSPF), Roots Approxiator (RA), and Numerically Controlled Oscillator (NCO). The block diagram of the complete system is shown in the Fig1. The system performs using uniform sampling with moderate sampling frequency. The phase resolution of the system is a function of applied sampling

frequency. The proposed DPLL performs in piece-wise manner, it accepts signal samples for one symbol period at a time, and does the further processing as described in the following subsections.

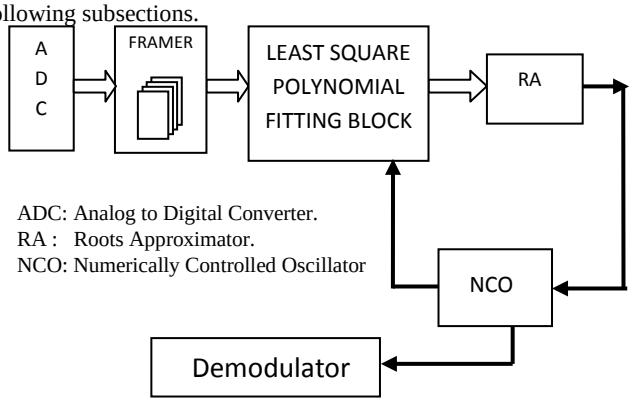

Fig 1: Block diagram of proposed DPLL

2.1 Least Square Polynomial Fitting block (LSPF)

We are replacing the traditional Phase Frequency Detector (PFD) of a DPLL with Least Square Polynomial Fitting Block (LSPF) because it can take care of functionalities of two major components of a traditional DPLL, namely signal conditioning and phase frequency detection. It has two inputs, the frequency count of local reference signal and the other one is the incoming input signal.

We have implemented a 6^{th} order polynomial fitting algorithm to fit the incoming signal to a signal with minimum distortion as replacement of anti-aliasing filter. The use of least-squares (LS) polynomial fitting filters to reduce random noise in time or wavelength variant analytical data has become widespread in the 20 years since Savitzky and Golay published the concept [9, 10]. The polynomial fitting method can eliminate the phase noise in the continuous interval. In addition to applying of these filters for increasing signal-to-noise ratio (SNR) with minimum signal distortion, they are also extremely useful in the numerical differentiation of data, producing results which are relatively insensitive to high-frequency noise. The proposed DPLL is designed to evaluate its performance under faded wireless transmission. So it is expected that at the receiver it will get multiple copies of faded signals with varying phase and noise. The requirement is a distortion less filtered signal with sharp zero crossing as we are applying polynomial root approximation algorithm for phase frequency detection.

Observed faded noisy signal by simulation was fitted by polynomial functions of different orders using least-squares linear regression (LSLR) method. We have found that the sixth order polynomial fitting can generate a good estimate of the sinusoid signal under effect of additive noise and multipath path fading channel.

The coefficients of best fit polynomial function of the noisy faded signal are measures of the Phase and Frequency associated with that signal. The theory associated with LSPF have been discussed briefly below.

If it is known that the measured quantity y is a linear function of t.

$$y = a_0 + a_1 t \tag{1}$$

The most probable values of a_0 (intercept) and a_1 (slope) can be estimated from a set of n pairs of experimental data $(t_1, y_1), (t_2, y_2), \ldots (t_n, y_n)$, where y- values are contaminated with a normally distributed - zero mean random error (e.g. random amplitudes, phases). This estimation is known as least-squares linear regression.

By implementing this analysis, it is easy to fit any polynomial of degree m to signal data $(t_1, y_1), (t_2, y_2), \ldots (t_n, y_n)$, (provided that $n \geq m + 1$) so that the sum of squared residuals S is minimized

$$y = a_0 + a_1 t + \cdots a_{m-1} t^{m-1} + a_m t^m \tag{2}$$

$$S = \sum_{i=1}^{n} [\mathrm{y_i} - (a_0 + a_1 t_i + \ldots a_m t_i^{\mathrm{m}})]^2 \tag{3}$$

By obtaining the partial derivatives of S with respect to $a_0, a_1, .., a_m$ and equating these derivatives to zero, the following system of $m-$equations and $m-$unknowns $(a_0, a_1, .., a_m)$ are defined:

$$\begin{aligned} & s_0 a_0 + s_1 a_1 + \cdots + s_m a_m = p_0 \\ & s_1 a_0 + s_2 a_1 + \cdots + s_{m+1} a_m = p_0 \\ & \ldots\ldots\ldots\ldots\ldots\ldots\ldots\ldots \\ & s_m a_0 + s_{m+1} a_1 + \cdots + s_{2m} a_m = p_m \end{aligned} \tag{4}$$

where,

$$s_k = \sum_{i=1}^{n} t_i^k \quad p_k = \sum_{i=1}^{n} y_i t_i^k \quad s_0 = n$$

This system is known a system of normal equations. The set of coefficients: $a_0, a_1, .., a_m$ is the unique solution of this system. For, $m = 1$ the familiar expressions used in linear least-square fit are obtained:

$$a_0 = \frac{\sum_{i=1}^{n} t_i^2 \sum_{i=1}^{n} y_i - \sum_{i=1}^{n} t_i \sum_{i=1}^{n} y_i t_i}{n \sum_{i=1}^{n} t_i^2 - \left(\sum_{i=1}^{n} t_i \right)^2} \quad \text{and}$$

$$a_1 = \frac{n \sum_{i=1}^{n} y_i t_i - \sum_{i=1}^{n} t_i \sum_{i=1}^{n} y_i}{n \sum_{i=1}^{n} t_i^2 - \left(\sum_{i=1}^{n} t_i \right)^2} \tag{5}$$

Similar expressions are obtained for coefficients of polynomials of higher degrees. The system of normal equations is set and the solution vector of $a_0, a_1, .., a_m$ coefficients is calculated.

LSPF does three jobs. *First*, it equates the coefficients of best fit polynomial function to the incoming faded signal. *Second*, with the use of the coefficients of polynomial function it generates the best fit signal samples free from ripples. *Third*, LSPF feeds the value the coefficients of best fit polynomial function and the frequency count of local reference signal to Roots Approximator (RA) for further processing.

2.2 Roots Approximator (RA)

The Root Approximator (RA) is the next major component in the proposed DPLL. It takes the value of the coefficients of best fit polynomial function and computes the roots of that polynomial function.

Given an m^{th} degree polynomial, the roots can be found by finding the eigenvalues $\boldsymbol{\lambda_i}$ of the following matrix.

$$\begin{bmatrix} -a_1/a_0 & -a_2/a_0 & -a_3/a_0 & \cdots & -a_m/a_0 \\ 1 & 0 & 0 & \cdots & 0 \\ 0 & 1 & 0 & \cdots & 0 \\ \vdots & \vdots & \vdots & \ddots & \vdots \\ 0 & 0 & 0 & \cdots & 0 \end{bmatrix} \quad (6)$$

And then crossponding roots can be computed by the following formula,

$$r_i = 1/\lambda_i \quad (7)$$

Roots of the polynomial function carries the phase and frequency information of the fitted signal. After evaluting the roots, the RA performs three additional jobs. It arrange the roots in ascending order and calculates the time period of fitted signlas from diffrence of any two alternate sorted roots values. From this time period RA calculates the the frequency associated with fitted signal and stores in a variable say "FREQUENCY_COUNT". Among the sorted roots RA computes the first positive to negative zero crossing root, which signifies the phase associated with fitted signal samples and stores in a variable say "PHASE_COUNT". As RA already having the information regarding frequency count of local reference signal, it compares this with new frequency count and based on this comparison it SET's or RESET's a flag say "FLAG_CH_FRQ". The status of this variable helps NCO to decide whether to change the local reference signal's frequency or not. RA feeds these three information namely "FREQUENCY_COUNT", "PHASE_COUNT" and "FLAG_CH_FRQ" to NCO for further processing.

2.3 Numerically Controlled Oscillator (NCO)

Numerically controlled oscillator (NCO) takes phase and frequency information from RA as input and adjust its local reference signal's phase and frequency and outputs a new reference signal.

As the DPLL is proposed for QPSK modulation scheme, it is expected that the frequency of the signal will not vary much, only the phase of the carrier associated with each symbol will vary, so we propose a new type of NCO having two outputs. The first output will be frequency corrected zero phased sinusoidal signal, and the second output will be frequency as well as phase corrected signal which will be applied as demodulator input.

Frequency adjustment algorithm we have applied is as follows:

1. NCO checks the status of the flags "FLAG_CH_FRQ". If its value is SET then step 2 to 4 is executed otherwise local reference signal's frequency remains same.
2. RA provides the information about frequency count via variable "FREQUENCY_COUNT".
3. NCO generates samples of new sinusoidal signal with frequency equal to "FREQUENCY_COUNT". This new "FREQUENCY_COUNT" will act as new reference input signal for the LSPF.

Phase adjustment algorithm we have applied is as follows:

1. After the frequency been adjusted, the time index of first positive to negative zero crossing of this new reference signal is stored in a variable say, "REF_PNC_COUNT".
2. RA provides index of first positive to negative zero crossing root of its input signal via a variable say, "PHASE_COUNT".
3. NCO changes the phase of local reference signal based on the value of the difference "REF_PNC_COUNT - PHASE_COUNT" stored in a variable say, "CHANGE_P_COUNT"
4. Having got the time delay information, the phase of the new frequency corrected reference signal is matched with that of input signal frame by the implementing array Left-shift / Right shift algorithm.
5. End of this shifting algorithm, we have a second version of the NCO output, which is phase and frequency matched to that of the input signal sample frame. This output is applied to the demodulation and decision block.

3. BACKGROUND PRINCIPLES

In this work involves the study of QPSK and Nakagami -*m* fading channels which are considered for the implementation as part of the work. The following subsections provide certain theoretical aspects of QPSK and Nakagami -*m* fading channels.

3.1 QPSK Signal Modeling

We have chosen QPSK signal modulation scheme in order to evaluate the performance of the proposed DPLL. QPSK is the most widely used phase modulation scheme and has applications that range from voice-band modems to high-speed satellite transmissions. The QPSK signals are defined as follows:

$$s_i(t) = A\cos(2\pi f_c t + \theta_i), \quad (8)$$

$$0 \le t \le T, \quad i = 1,2,3,4$$

where $\theta_i = \dfrac{(2i-1)\pi}{4}$

The four available phases are therefore $\frac{\pi}{4}, \frac{3\pi}{4}, \frac{5\pi}{4}, \frac{7\pi}{4}$.

3.2 Nakagami-m Fading Channel

The proposed DPLL is designed to investigate its performance over wireless multipath under severe to less fading conditions coupled with additive noise. Radio waves propagate from transmitting antenna and travel through free space undergoing

absorption, reflection, diffraction and scattering. They are greatly affected by ground, buildings, trees and other object which exists in their path. All these things are responsible for the characteristics of the received signal.

The Rayleigh and Racian fading models fall short of describing long distance fading effects with sufficient accuracy. The model proposed by Nakagami uses an adaptive parameter to fading conditions. Using Nakagami fading model, the fading condition more or less severe than the Rayleigh and Racian fading can be accurately modeled [11, 12]. Nakagami Fading assumes that the transmitted signal that has pass through the channel will fade according to Nakagami distribution. Nakagami Fading occurs for multipath scattering with relatively larger time-delay spreads, with different clusters of reflected waves. If the delay times are significantly exceed the bit period of digital link, the different clusters produce serious intersymbol interference. The probability distribution function of Nakagami-*m* distribution is given by:

$$p(r)=\frac{2}{\Gamma(m(h))}\left(\frac{m(h)}{\Omega_p}\right)^{m(h)} r^{2m(h)-1}\exp\left(-\frac{m(h)r^2}{\Omega_p}\right) \quad (9)$$

Where r is Nakagami envelope, $\Gamma(.)$ is a gamma function, $\Omega_p = E\left(r^2\right)$ is the instantaneous power and $m(h)=\frac{E(r^2)}{\mathrm{var}(r^2)}$, the fading figure or shape factor.

1. If the envelope is Nakagami distributed, the corresponding power is Gamma distributed.
2. In the special case $m(h)=1$, Rayleigh fading is recovered, with an exponentially distributed instantaneous power.
3. For $m(h) > 1$, the fluctuations of the signal strength are reduced as compared to Rayleigh Fading.
4. For $m(h)=0.5$, it becomes one-sided Gaussian distribution.
5. For $m(h)=\infty$, the distribution becomes impulse i.e. no fading. The sum of multiple independent and identically distributed Rayleigh-fading signals has Nakagami Distributed signal amplitude.

We have used Sum-of-Sinusoids Technique to generate Nakagami – *m* fading samples. Let h(t) be the Nakagami – *m* fading samples, x(t) be the transmitted signal sample and a(t) be the AWGN, then the received signal sample r(t) can be given by

$$r(t)=x(t)h(t)+a(t) \quad (10)$$

To evaluate the first order statistics of the received signal, we have to decompose signal to inphase and quadrature component, and we can write

$$r(t)=r_I(t)\cos\omega_c t + r_Q(t)\sin\omega_c t \quad (11)$$

The envelope of the received signal can be given by

$$Y=\sqrt{r_I(t)^2+r_Q(t)^2} \quad (12)$$

Corresponding Nakagami parameter can be measured by following equations.

Instantaneous power of received signal $\Omega_p = E\left(Y^2\right)$ (13)

and fading figure or shape factor can measured from

$$m(r)=\frac{E\left(Y^2\right)}{E\left(\left(Y^2-E\left(Y^2\right)\right)^2\right)} \quad (14)$$

The probability distribution function of the received signal can now be obtained from (9).

Using equation (10) received signal with Nakagami parameter $m(r) \geq 1$ can only be generated. For generating received signal with $0.5 \leq m(r) \leq 1$, we have followed the following equation

$$r(t)=\left(x(t)h(t)\right)h(t)+a(t) \quad (15)$$

To statistically characterize fading channel, two quantities the level-crossing rates (LCRs) and average fade durations (AFDs**)** reflect the scattering environment, and thus are called the second-order statistics of a fading channel. The LCR is defined as the number of times per second that the envelope of fading channel crosses a specified level Y_0 in a positive-going direction, the AFD, is defined **as** the average period of time for which the received signal is below a specified level Y_0.If Y' be the rate of change of the envelope, then average number of positive zero crossings can be given by the equation [12].

$$N_{Y_o}=\int_0^\infty Y' p\left(Y_0, Y'\right)dY' \quad (16)$$

And it can be rewritten as

$$N_{Y_o}=\frac{2\sigma Y'}{\sqrt{2\pi}\Gamma(m(r))}\left(\frac{m(r)}{\Omega_p}\right)^{m(r)} Y_0^{2m(r)-1}\exp\left(-\frac{m(r)Y_0^2}{\Omega_p}\right) \quad (17)$$

The average fade duration obtained from the following expression [12]

$$\tau_Y=\frac{1}{\Gamma(m(r))N_{Y_o}}\gamma\left(m(r);\frac{m(r)}{\Omega_p}Y_0^2\right) \quad (18)$$

where, $\gamma\left(m(r);\frac{m(r)}{\omega_p}Y_0^2\right)$ is the incomplete gamma function.

4. EXPERIMENTAL CONSIDERATIONS

After testing each block independently as described above, a simulation model is created integrating each block which models a complete communication scenario. QPSK is signal generated by modulating a sufficient numbers of random binary bits with a carrier and transmitted over Nakagami fading channel under various fading conditions. At receiver, received analog signal is converted to digital form. Frame of received data corresponding to one symbol period is passed through Least Square Polynomial Fitting Block (LSPF) one by one, which fits the received data frame to best fit signal sample using 6^{th} degree polynomial approximation using LS method. Output of LSPF block is feeds to the Root Approximator (RA). RA equates the set of roots of the best fit polynomial function and feeds to NCO. Based on the roots, NCO produces two outputs, one the frequency adjusted signal that is applied to PFD as new reference signal and the other, the phase frequency corrected signal that is applied to QPSK demodulator block. QPSK demodulator recovers the incoming signal frame to binary bits. Last and the final block is the BER calculation. It has two inputs, one is the modulating random binary bits from QPSK modulator and the other is the demodulated binary bits from QPSK demodulator. This block counts number of error that taken place.

Table 1: The Nakagami fading figure *m(r)* of received signal, number of error bits counted and received signal power for various combinations of Nakagami Channel fading figure *m(h)=0.5* and SNR for 5000 transmitted bits with signal frequency 900 MHz and sampling frequency 9 GHz.

m(h)	Received SNR dB	Received Signal *m(r)*	Power Ω_p	Number of Error Bit Occurred
0.50	-20	1.01	18.9	2088
0.50	-15	1.04	6.1	1718
0.50	-10	1.07	2.2	1161
0.50	-5	1.13	1.0	721
0.50	0	1.22	0.6	314
0.50	5	1.40	0.4	125
0.50	10	1.51	0.4	63
0.50	15	1.54	0.4	24
0.50	20	1.58	0.4	12

Table 2: The Nakagami fading figure *m(r)* of received signal, number of error bits counted and received signal power for various combinations of Nakagami Channel fading figure *m(h)=1.0* and SNR for 5000 transmitted bits with signal frequency 900 MHz and sampling frequency 9 GHz.

m(h)	Received SNR dB	Received Signal *m(r)*	Power Ω_p	Number of Error Bit Occurred
1.00	-20	1.00	37.7	1956
1.00	-15	1.02	12.6	1614
1.00	-10	1.08	4.5	1076
1.00	-5	1.11	2.0	566
1.00	0	1.14	1.2	215
1.00	5	2.00	1.0	95
1.00	10	2.50	0.9	36
1.00	15	2.60	0.8	10
1.00	20	2.70	0.7	5

Table 3: The Nakagami fading figure *m(r)* of received signal, number of error bits counted and received signal power for various combinations of Nakagami Channel fading figure *m(h)=2.0* and SNR for 5000 transmitted bits with signal frequency 900 MHz and sampling frequency 9 GHz.

m(h)	Received SNR dB	Received Signal *m(r)*	Power Ω_p	Number of Error Bit Occurred
2.00	-20	1.00	37.5	1722
2.00	-15	1.02	12.3	1508
2.00	-10	1.08	4.6	877
2.00	-5	1.21	2.0	322
2.00	0	1.62	1.2	121
2.00	5	2.61	1.0	45
2.00	10	3.73	0.9	23
2.00	15	4.10	0.9	7
2.00	20	4.52	0.9	4

Table 4: The Nakagami fading figure *m(r)* of received signal with $0.5 \leq m(r) \leq 1$, number of error bits counted and received signal power for various combinations of Nakagami Channel fading figure *m(h)=0.5* and SNR for 5000 transmitted bits with signal frequency 900 MHz and sampling frequency 9 GHz.

m(h)	Received SNR dB	Received Signal *m(r)*	Power Ω_p	Number of Error Bit Occurred
0.50	-5	0.7436	1.91	937
0.50	0	0.6434	0.69	622
0.50	2	0.5827	0.61	426

5. RESULTS AND DICUSSION

The system has been simulated for counting bit errors occurred during reception and demodulation of 5000 transmitted random binary bits with carrier frequency 900 *MHz.* We have generated different sets of Nakagami distributed numbers representing various fading conditions with value of *m(h)*, the fading figure have been chosen to be *0.5,1.0, 2.0,* and *3.0*. Then, each of these sets is multiplied with signal samples to result faded signal sets of different fading figure. Now to each of the faded signal set AWGN white noise is added with SNR value ranging from *-20dB* to *20dB* to produce further multiple sets of faded noisy signal sets, each representing combination of different fading figure and different SNR of received signal. Finally for each of the resultant faded noisy signal sets, the Nakagami fading figure *m(r)*, the instantaneous power ω_p is calculated and passed through the DPLL and corresponding Bit Error is counted. Table 1-3 shows the Nakagami fading figure *m(r)* of the received signal, number of error bits counted and received signal's instantaneous power Ω_p for various combinations of Nakagami channel fading figure *m(h)* and SNR for 5000 transmitted bits with signal frequency 900 MHz and sampling frequency 9GHz..

Received signal PDF for various channel fading figures *m(h)* and different SNRs are represented by the plots shown in Figs 2 to 5. The corresponding plots of LCR are represented by Figs 6 to 9. It is clear from the figures that with increase of $m(r)$, which means improvement in the propagation environment, the LCR gradually decreases. The AFD plots are represented by Figs 10 to 13. From the plots, we can conclude that the AFD at low signal level will decrease with the increase of m(r). On the other hand, the AFD in high signal level will increase with the increase of m(r). Using equation (15) we have generated the received signal with Nakagami fading figure $m(r) < 1$, which represents severe fading conditions. The results derived are shown in Table 4 and corresponding plots of received signal's PDF are shown in Fig.14.

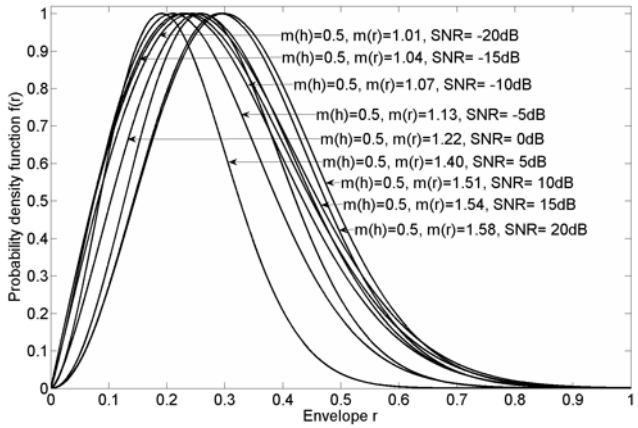

Fig.2: Received signal PDF for channel fading figure *m(h)=0.5* and different SNR for 5000 transmitted bits with signal frequency 900 MHz.

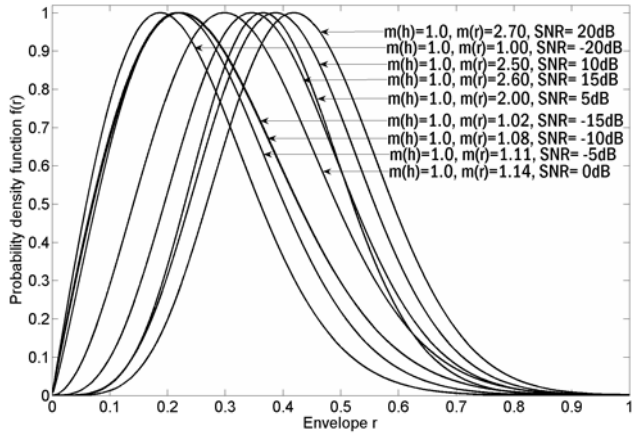

Fig.3: Received signal PDF for channel fading figure *m(h)=1* and different SNR for 5000 transmitted bits with signal frequency 900 MHz.

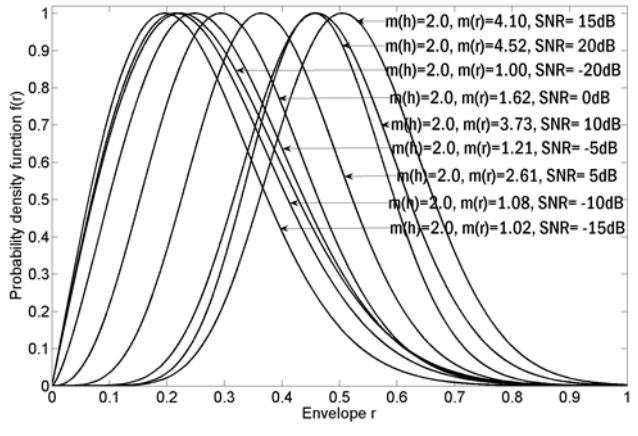

Fig.5: Received signal PDF for channel fading figure *m(h)=2.0* and different SNR for 5000 transmitted bits with signal frequency 900 MHz

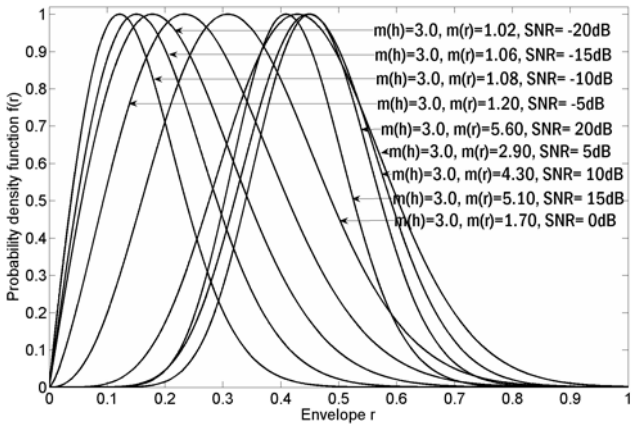

Fig.5: Received signal PDF for channel fading figure *m(h)=3.0* and different SNR for 5000 transmitted bits with signal frequency 900 MHz.

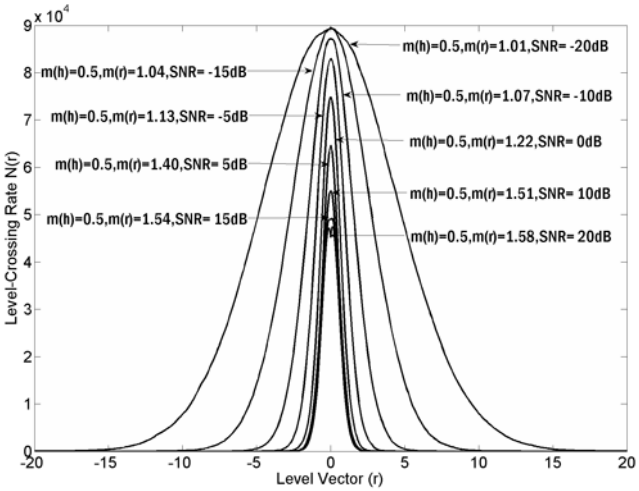

Fig.6: Plot of LCR for channel fading figure *m(h)=0.5* and different SNR for 5000 transmitted bits with signal frequency 900 MHz.

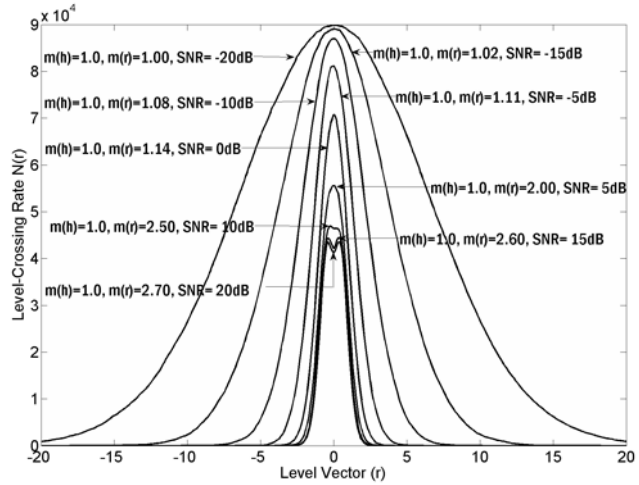

Fig.7: Plot of LCR for channel fading figure *m(h)=1.0* and different SNR for 5000 transmitted bits with signal frequency 900 MHz.

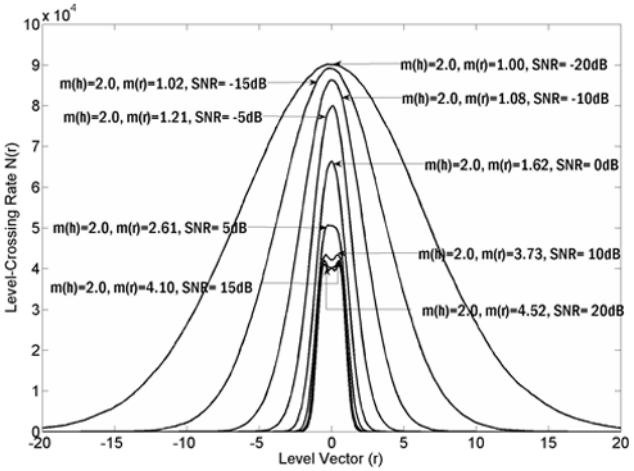

Fig.8: Plot of LCR for channel fading figure *m(h)=2.0* and different SNR for 5000 transmitted bits with signal frequency 900 MHz.

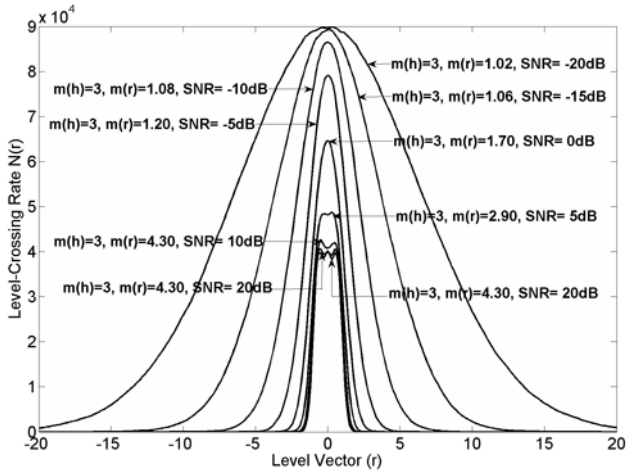

Fig.9: Plot of LCR for channel fading figure *m(h)=3.0* and different SNR for 5000 transmitted bits with signal frequency 900 MHz.

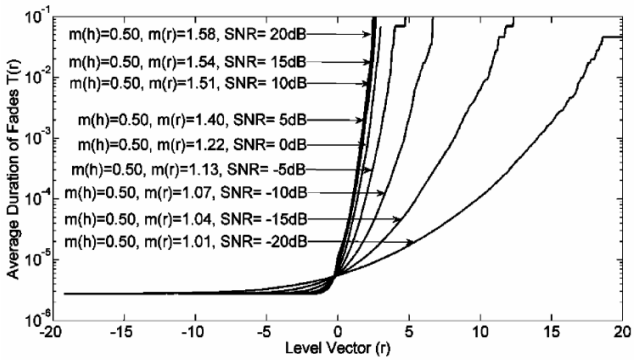

Fig.10: Plot of AFD for channel fading figure *m(h)=0.50* and different SNR for 5000 transmitted bits with signal frequency 900 MHz.

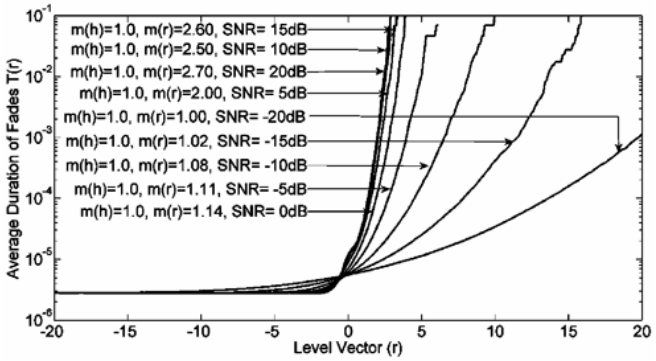

Fig.11: Plot of AFD for channel fading figure *m(h)=1.0* and different SNR for 5000 transmitted bits with signal frequency 900 MHz.

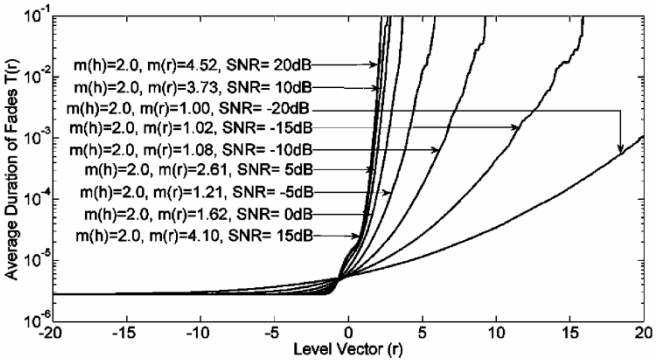

Fig.12: Plot of AFD for channel fading figure *m(h)=2.0* and different SNR for 5000 transmitted bits with signal frequency 900 MHz.

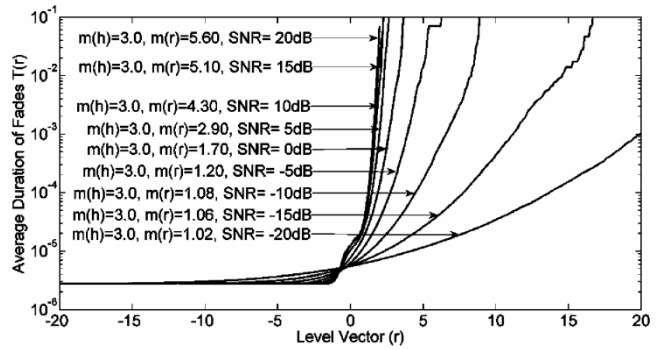

Fig.13: Plot of AFD for channel fading figure *m(h)=3.0* and different SNR for 5000 transmitted bits with signal frequency 900 MHz.

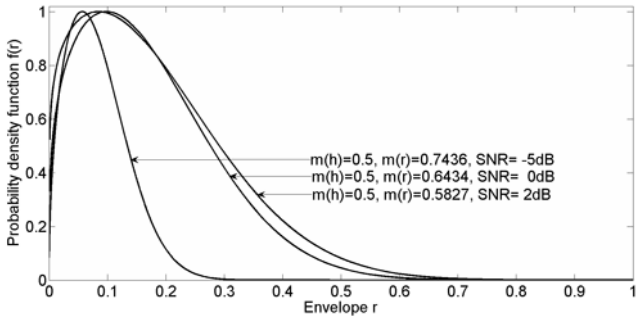

Fig.14: PDF of received signal with Nakagami fading figure $m(r) < 1$

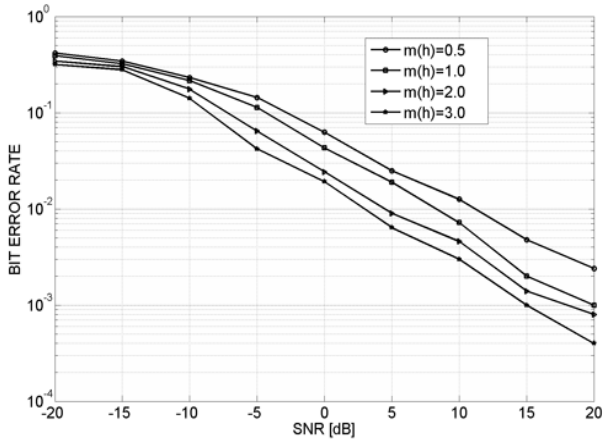

Fig.15: BER Vs SNR Plot for various combinations of channel fading figure *m(h)* and SNR for 5000 transmitted bits with signal frequency 900 MHz and sampling frequency 9 GHz.

Bit error rate performance of the DPLL is represented by a BER VS SNR plot Fig.15 for various values of Nakagami fading figure *m(h)* of Nakagami channel. In recent years, the result of BER analysis for QPSK signaling in Nakagami fading channel has been reported by a few authors [13, 14, 15]. In their results a BER of the order of above 0.1 at SNR 0dB have been reported. In comparison to such works, we have found that our system is able to attain a BER of below 0.1 at SNR 0 dB for a carrier frequency of 900 MHz and at a sampling frequency of 9 GHz.

We have also noticed that with further increase of sampling frequency, the BER performance gets even better. Thus, the proposed DPLL provides satisfactory performance in Nakagami –m fading channel with QPSK signal using a carrier frequency 900 MHz with sampling frequency 9 GHz.

6. CONCLUSION

In this paper, we have analyzed the performance of modified structure of a DPLL for carrier detection under various fading conditions. The implementation of modified structure of a DPLL for carrier detection in Nakagami –*m* fading channel has also been discussed. For phase frequency detection LSPF algorithm have been implemented which replaces the two major components of traditional DPLL, namely the Phase Frequency Detector and Loop Filter. Especially, we have generated moderately to severely faded signal using Nakagami channel model, as input to the proposed DPLL. Statistical characteristics of the received signal have been evaluated in terms of PDF, LCR and AFD. Results show improvement in carrier detection over existing methods. This work can be extended further by applying some coding techniques to improve the BER performance of the system.

7. REFERENCES

[1] Fahim, A. M. and Elmasry, M. I. 2003. A Fast Lock Digital Phase-Locked-Loop Architecture for Wireless Applications, IEEE Transactions on Circuits and systems-II: Analog and digital signal processing, vol.50, no. 2, Feb., 2003.

[2] Saber, M., Jitsumatsu,Y. and Khan, M.T.A. 2010. Design and Implementation of Low Power Digital Phase-Locked Loop, Proceedings of the ISITA2010, Taichun, Taiwan, pp. 928 – 933, Oct., 2010.

[3] Stefan, M. and Christian, V. 2008. Improved lock-time in all-digital phase-locked loops due to binary search acquisition, Proceedings of the 15th IEEE International Conference on Electronics, Circuits and Systems, ICECS 2008, Malta, pp. 384-387, 2008.

[4] Staszewski, R. B. and Balsara, P. T. 2005. Phase-Domain All-Digital Phase-Locked Loop, IEEE transactions on Circuits and Systems—II: Express Briefs, vol. 52, no. 3, Mar., 2005.

[5] Gill, G.S. and Gupta, S.C. 1972. First-order discrete phase-locked loop with applications to demodulation of angle-modulated carrier, IEEE Trans,. Commun. Technol., vol. COM-20, pp. 454-462, Jun., 1972.

[6] Elnoubi, S.M. and Gupta, S.C. 1985. Performance of First-order digital Phase-Locked Loops in Mobile Radio Communication, IEEE Trans,. Commun., vol. COM-33, pp, 450-456, May 1985

[7] Suzuki, H. 1977. A statistical model for urban multipath propagation, IEEE Trans. Commun., vol. COM-25, pp. 673–680, Jul., 1977.

[8] Luo, J X and Zeidler, J R. 2000. A Statistical Simulation Model for Correlated Nakagami Fading Channel, Proceedings of the, International Conference on Communications Technology 2000,. Beijing, China. Vol.2 pp. 1680-1684, Aug., 2000.

[9] Savitzky, A. and Golay, MJE. 1972. Smoothing and Differentiation of Data by Simplified Least Squares Procedures, Analytical Chemistry, vol. 44, pp. 1906-1909, 1972.

[10] Leach, R. A., Carter, C. A. and Harris, J. M. 1984. A Least-Squares Polynomial Filters for Initial Point and Slope Estimation, Anal. Chem., vol. 56, no. 13, pp. 2304–2307, 1984.

[11] Nakagami, M. 1960. The m-distribution-A general formula of intensity distribution of rapid fading, in Statistical Methods in Radio Wave Propagation**,** W.C. Hoffman, Ed.New York: pergamon, pp.3-36, 1960.

[12] Youssef, N., Munakata T. and Takeda M. 1996 Fade Statistics in Nakagami Environments, IEEE Trans., vol. 8, no. 96, pp. 7803–3567, 1996.

[13] Sood, N., Sharma, A.K. and Uddin, M. 2010. BER Performance of OFDM-BPSK and -QPSK Over Generalized Gamma Fading Channel, International Journal of Computer Applications, vol. 3, no.6, pp. 13-16, June 2010.

[14] Smadi, M. A. 2009. Performance Analysis of QPSK System with Nakagami Fading Using Efficient Numerical Approach, Proceedings of IEEE 9th Malaysia International Conference on Communications, Kuala Lumpur, Malaysia, pp. 447-450, December 2009.

[15] Cheng, J., Beaulieu, N. C. and Zhang, X. 2005. Precise BER Analysis of Dual-Channel Reception of QPSK in Nakagami Fading and Cochannel Interference, IEEE Communications Letters, vol. 9, no. 4, pp. 316–318, April 2005.